



# Audio Engineering Society Convention Paper

Presented at the 114th Convention  
2003 March 22–25 Amsterdam, The Netherlands

*This convention paper has been reproduced from the author's advance manuscript, without editing, corrections, or consideration by the Review Board. The AES takes no responsibility for the contents. Additional papers may be obtained by sending request and remittance to Audio Engineering Society, 60 East 42<sup>nd</sup> Street, New York, New York 10165-2520, USA; also see [www.aes.org](http://www.aes.org). All rights reserved. Reproduction of this paper, or any portion thereof, is not permitted without direct permission from the Journal of the Audio Engineering Society.*

---

## The Full-Sphere Sound Field of Constant Beamwidth Transducer (CBT) Loudspeaker Line Arrays

D. B. (Don) Keele, Jr.

*Harman/Becker Automotive Systems  
1201 South Ohio St.  
Martinsville, IN 46151  
USA  
E-mail: [DKeele@Harman.com](mailto:DKeele@Harman.com)*

### ABSTRACT

The full-sphere sound radiation pattern of the CBT circular-wedge curved-line loudspeaker array exhibits a 3D petal-or eye-shaped sound radiation pattern that stays surprisingly uniform with frequency. Oriented vertically, it not only exhibits the expected uniform control of vertical coverage but also provides significant coverage control horizontally. The horizontal control is provided by a vertical coverage that smoothly decreases as a function of the horizontal off-axis angle and reaches a minimum at right angles to the primary listening axis. This is in contrast to a straight-line array that exhibits a 3D sound field that is axially symmetric about its vertical axis and exhibits only minimal directivity in the horizontal plane due to the inherent directional characteristics of each of the sources that make up the array.

### 1. INTRODUCTION

Constant beamwidth transducer (CBT) array theory is based on un-classified military under-water transducer research done in the late 1970s and early 80s [1, 2]. The research describes a curved-surface transducer in the form of a spherical cap with frequency-independent Legendre shading that provides wide-band extremely-constant beamwidth and directivity behavior with virtually no side lobes. The theory was applied to loudspeaker arrays by

Keele in 2000 [3] where he extended the concept to arrays based on toroid-shaped curved surfaces and to circular-arc line arrays. Keele also extended the concept to straight-line and flat-panel CBT arrays with the use of signal delays [4]. Section 8: Appendix 1 contains a brief review of CBT theory.

Traditionally, line arrays are thought to provide directional control in one plane only. This is quite true for straight-line arrays but not true for curved-line arrays. In addition to the expected coverage control in the plane of the curved array, the curvature of the line array also provides directional control at off-axis angles in the opposite planes. For the typical vertical-oriented curved-line array, this means that the array provides the expected directional control vertically but also provides control horizontally.

The horizontal directional control provided by the curvature of the line array is primarily exhibited by a narrowing vertical coverage as a function of the horizontal off-axis angle and an increasing level as the listener location proceeds off axis horizontally. In front of the curved-line array, along the primary listening axis, the curvature of the array places sources at different distances from the listening location and provides the primary directional-control mechanism. However, for off-axis horizontal locations, the curvature of the array is less and less evident as one proceeds to greater off-axis horizontal angles. At  $\pm 90^\circ$  off-axis horizontally, the curvature is entirely nullified and all sources are essentially equidistant from far-field listening or observation locations. At these locations, the array essentially appears as a straight-line array which provides both maximum level and the narrowest possible vertical coverage. Interestingly, the curved-line array thus provides its maximum intensity at right angles to its primary listening axis.

Further analysis of the CBT circular-wedge line array reveals that its vertical coverage gets narrower and narrower as one proceeds off-axis horizontally. The narrowing of vertical coverage is found to follow the cosine of the off-axis horizontal angle. This means that the vertical coverage of the array smoothly narrows from its designed on axis value and reaches a minimum at right angles horizontal to the primary listening axis.

The full-sphere sound field of the CBT curved-line array reveals a characteristic 3D petal- or eye-shaped sound radiation pattern which stays surprisingly uniform with frequency. This provides very uniform directivity and beamwidth control above a certain frequency set by the size of the array and its designed vertical coverage. Although the horizontal  $\pm 90^\circ$  off-axis intensity is higher than the primary designed listening axis, the effect is essentially negated

because the vertical coverage of the array is narrowest at these same extreme off-axis angles.

This paper is organized as follows: Section 2 has a description of the numerical simulator used to predict the radiation patterns of the modeled arrays, describes typical simulator outputs, and describes the 3D axis and orientation for the polar balloon plots. Section 3 analyzes the predicted sound field of a conventional straight-line array designed to provide a controlled vertical coverage. Section 4 analyzes the sound field of two curved-line CBT arrays: the first designed to provide broad vertical coverage, and the second designed for narrow vertical coverage. The variation of the CBT curved-line array's vertical beamwidth as a function of the array's horizontal (azimuth) angle is analyzed in section 5. Section 6 states the conclusion of the paper while section 7 lists its references. Sections 8 and 9 include appendices containing a review of CBT theory (Appendix 1), and a full set of polar balloons at octave center frequencies for both analyzed CBT arrays of Section 4 (Appendix 2).

## 2. ARRAY SIMULATOR

### 2.1. Description

The point-source array simulator program used in [3, 4] was used to predict the directional characteristics of the various arrays in this paper. This program calculates the pressure distribution at a specific distance (all simulations here are done at a far-field distance of 250m) for a 3-D array of point sources of arbitrary magnitude and phase.

Polar rotations were all done around the center of the coordinate system. Note that all the conventional curved CBT arrays were offset so that their centers of curvature coincided with the center of the coordinate system.

Program outputs include:

1. Source configuration views as seen from front, top, and sides.
2. Horizontal and vertical beamwidth (-6dB) vs. frequency plots at each one-third-octave center from 20 Hz to 16 kHz.
3. Directivity index and Q vs. frequency plots at each one-third-octave center from 20 Hz to 16 kHz.
4. On-axis frequency response (loss) plot vs. frequency (compared to all sources on and in-phase

at the pressure sampling point). This plot indicates how much on-axis attenuation the array imposes as compared to the situation where all the sources add in phase at the sampling point.

5. Complete set of 3D polar balloons showing oblique, front, side, and top views at octave center frequencies. These polar balloons show the predicted 3D sound field of an array with a shape based on a deformed sphere whose radius in a particular direction is proportional to the array's radiated level (in dB) in that particular direction. The shape is scaled linearly such that a radius of 1 corresponds to 0 dB, a radius of 0.5 corresponds to -20 dB, and a radius of 0 (the center) corresponds to a level of -40 dB.

## 2.2. Color Coding

The dB level of all the polar balloons in this paper are color coded in a yellow-hot scheme according to the following scale (Fig.1):

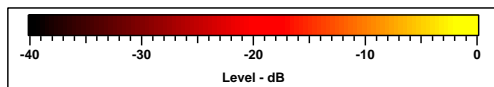


Fig. 1. Color scale used for the polar balloon plots in this paper. The scale varies smoothly from high-level yellow at 0 dB (right), through mid-level red at -20 dB, to low-level black at -40 dB.

## 2.3. Axis Orientation

This paper's 3D orthogonal axis system is shown in Fig. 2. All the arrays are constructed either on the Z axis (straight-line arrays) or on the X-Z plane (curved-line arrays) with their axis facing in the positive X direction.

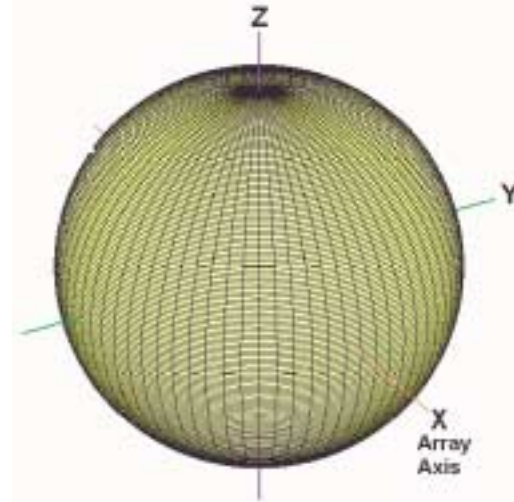


Fig. 2. Axis orientation for the oblique views of the polar balloon plots. The orientations are illustrated by the directional pattern of an omni-directional source (perfect spherical polar balloon). The orthogonal rectangular X-Y-Z axis are indicated. The axis are color coded as follows: X: red, Y: green, and Z (up-down): blue. The array's axis points in the direction of the positive X axis.

## 3. STRAIGHT-LINE ARRAY

To illustrate the directional pattern of a source that exhibits omni-directional radiation in one plane and directional radiation in the other, a straight-line array was analyzed. The array is composed of 50 point sources equally distributed along a 0.34m (13.5") distance on the Z axis centered on the X-Y plane. The array is one wavelength high at 1 kHz.

The strengths of the sources have been adjusted to follow a Hann (cosine squared) window with the center source on full and the strengths of the remaining sources smoothly tapering to zero at the outside ends of the array. This shading minimizes side lobes.

The close 6.8mm (0.27") spacing of the sources insures operation to above 20 kHz without grating lobes. Essentially this means that the line operates as a continuous source for frequencies below 20 kHz. Figures 3 to 5 respectively show side, front, and top views of the array.



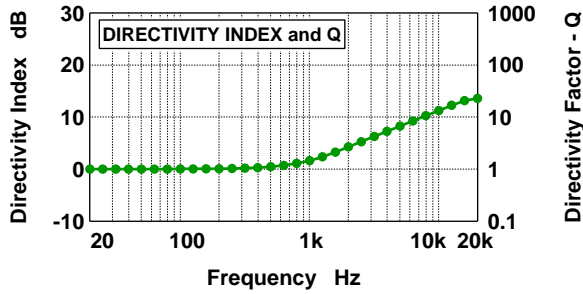


Fig. 7. Directivity index (left scale) and Q (right scale) of the array of Fig. 3. Note the increasing directivity above 1 kHz.

The on-axis loss of the array (essentially the on-axis frequency response) is shown in Fig. 8. The curve is normalized to the level which results when all sources are on (at their shaded level) and in-phase at the observation point. The straight-line array has no on-axis loss because all points of the array are essentially equidistant from a far-field point on its axis.

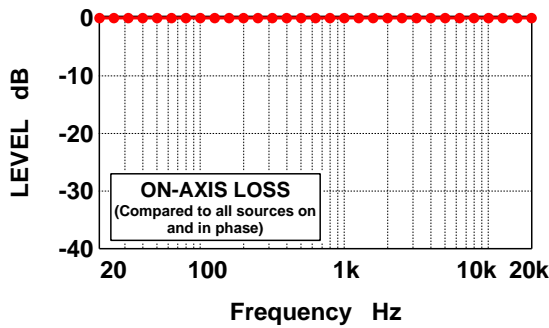


Fig. 8. On-axis loss of the array of Fig. 3.

### 3.1. Broad Vertical Coverage Balloon Plots of Straight-Line Array

The following polar balloons illustrate the 3D directional radiation of the line array of Fig. 3 at a frequency of 1.4 kHz where the array exhibits a broad vertical beamwidth of 90°. These balloons are generated by calculating the response every 10° in azimuth (longitude) and every 2.5° in elevation (latitude). Figures 9 – 11 show respectively oblique, front (also side), and top views of the balloon. Refer to Section 2 for a description of the balloons and their color coding.

Note that the different views of the balloon illustrate the omni-directional radiation of the array horizontally and the directional radiation vertically.

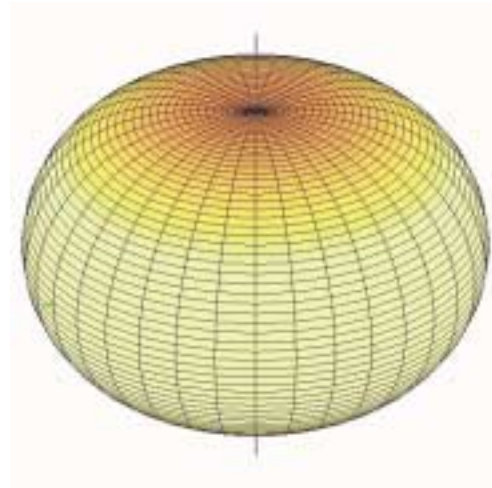


Fig. 9. Oblique view of the polar balloon of the straight-line array of Fig. 3 at 1.4 kHz where the vertical coverage is 90°. Refer to Fig. 2 for axis orientation.

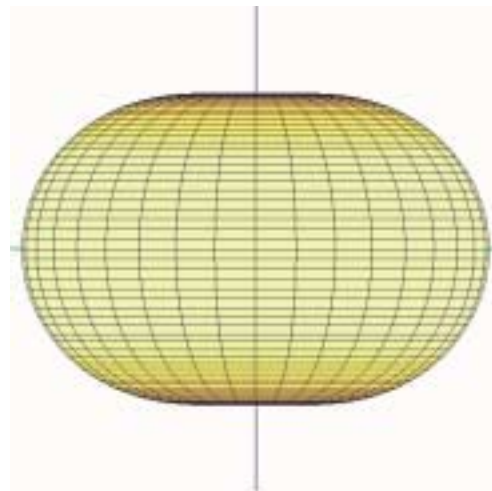


Fig. 10. Front (also side) view of the polar balloon of the straight-line array of Fig. 3 at 1.4 kHz. The X (also Y) axis points out of the page. Note the pumpkin shape in this view which indicates narrowing of the vertical coverage.

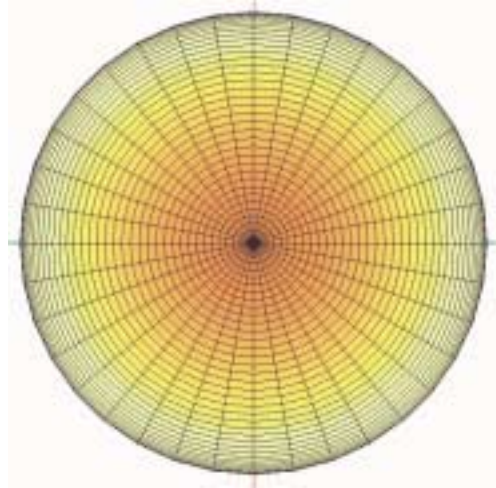


Fig. 11. Top view of the polar balloon of the straight-line array of Fig. 3 at 1.4 kHz. Note the omnidirectional (circular) horizontal radiation in this view. The Z axis points out of the page.

### 3.2. Narrow Vertical Coverage Balloon Plots of Straight-Line Array

The following polar balloons illustrate the 3D directional radiation of the line array of Fig. 3 at a frequency of 5.3 kHz where the array exhibits a narrow vertical beamwidth of  $22.5^\circ$ . These balloons are generated by calculating the response every  $10^\circ$  in azimuth (longitude) and every  $2.5^\circ$  in elevation (latitude). Figures 12 – 13 show respectively oblique, front (also side), and top views of the balloon. Refer to Fig. 1 for color coding of the balloons.

These different balloon views also illustrate the omnidirectional radiation of the array horizontally and the directional radiation vertically.

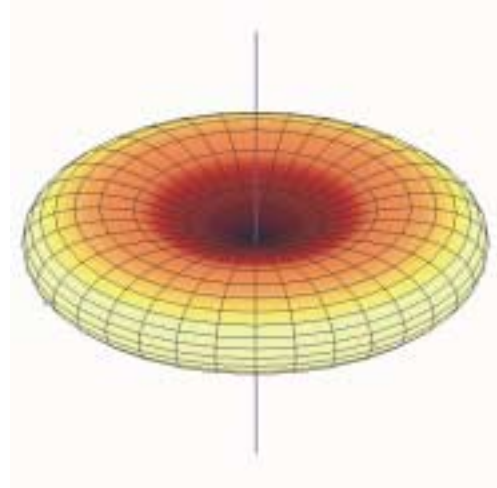


Fig. 12. Oblique view of the polar balloon of the straight-line array of Fig. 3 at 5.4 kHz where the vertical coverage is  $22.5^\circ$ . Refer to Fig. 2 for axis orientation. The donut shape of the polar balloon indicates omnidirectional horizontal radiation and narrow vertical radiation.

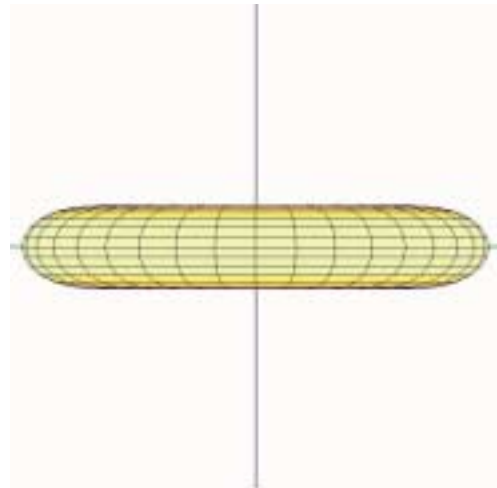


Fig. 13. Front (also side) view of the polar balloon of the straight-line array of Fig. 3 at 5.3 kHz. The X (also Y) axis points out of the page.

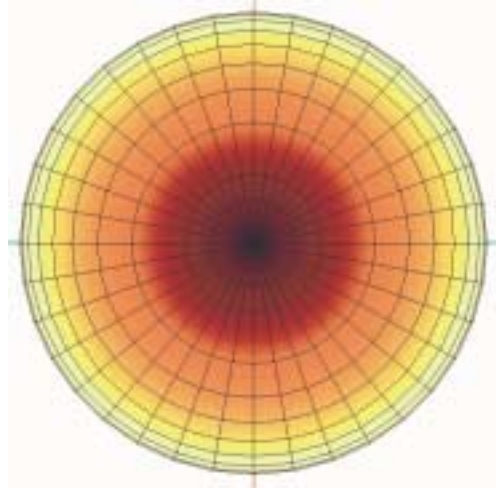


Fig. 14. Top view of the polar balloon of the straight-line array of Fig. 3 at 5.3 kHz. Note the omnidirectional (circular) horizontal radiation in this view.

#### 4. CURVED-LINE CBT ARRAYS

The directional patterns of curved-line CBT arrays exhibit varying vertical coverage but do not exhibit omnidirectional horizontal coverage. This is distinctly different than the behavior of the straight-line arrays. This behavior is investigated by analyzing the full-sphere radiation characteristics of two CBT curved-line arrays: one designed for a broad  $90^\circ$  vertical coverage and the other for a narrow  $22.5^\circ$  vertical coverage. These arrays are described in the following two sections.

##### 4.1. Broad Vertical Coverage CBT Array

This array is designed to provide a broad  $90^\circ$  vertical coverage on axis at frequencies above 1 kHz. As will be shown, the vertical coverage angle of the CBT curved-line array is not constant but changes as a function of the horizontal off-axis angle.

The array is composed of 50 point sources equally distributed around a  $140^\circ$  circular arc of 0.34m (13.5") height located on the Z-X plane. The center of curvature of the arc is located at the origin. The arc's radius is 182mm (7.18").

With Legendre shading (Eq. 1 and 3, Appendix 1) of the strengths of the point sources, this array will then exhibit an on-axis vertical beamwidth of roughly  $90^\circ$  which is roughly 64% of the arc angle ( $= 0.64 * 140^\circ$ ). As before, the array is one wavelength high at 1 kHz. Also as before, the close spacing of the sources insures that the line essentially behaves continuously up to 20 kHz.

Figures 15 to 17 respectively show side, front, and top views of the array.

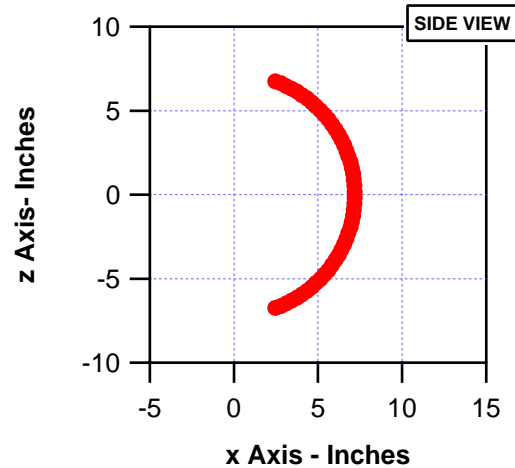


Fig. 15. Side view of the  $140^\circ$  CBT curved-line array providing a vertical coverage of  $90^\circ$  made up of 50 point sources. The array is 0.34m (13.5") high (one wavelength at 1 kHz). The array's center of curvature is located at the origin. The array points to the right in the direction of the positive X axis.

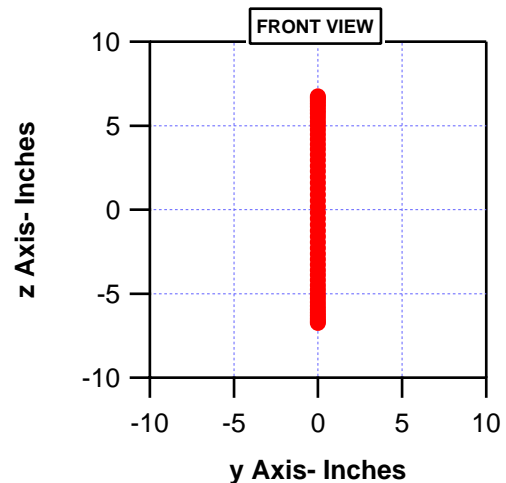


Fig. 16. Front view of the CBT array of Fig. 15.

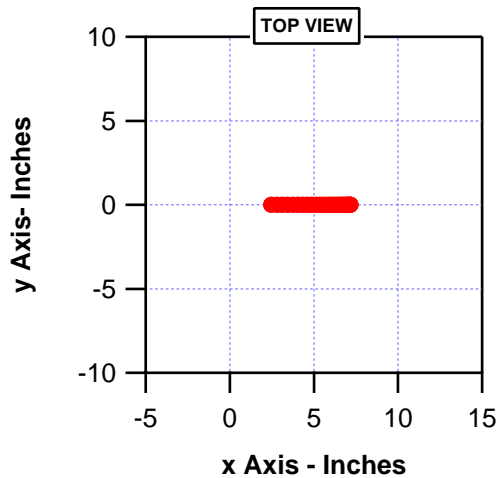


Fig. 17. Top view of the CBT array of Fig. 15.

Figure 18 shows the predicted vertical and horizontal beamwidth (-6 dB) of the array of CBT Fig. 15.. Note the extremely uniform vertical beamwidth of the array above 1 kHz. Although the horizontal beamwidth is constant at 360°, this does not imply that the horizontal coverage is independent of direction in the horizontal plane. This is in stark contrast to the behavior of the straight line array of Fig. 3. As will be shown shortly, the vertical beamwidth of the CBT curved-line array is a function of the horizontal (azimuth) angle.

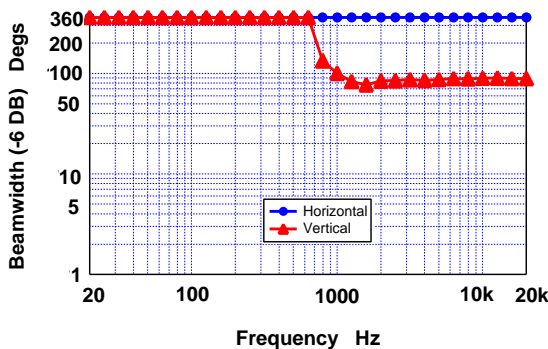


Fig. 18. Horizontal and vertical beamwidth (-6 dB) of the CBT array of Fig. 15.

Figure 19 indicates the CBT array’s predicted directivity. The directivity is quite uniform above 1 kHz, although exhibiting a low directivity index that remains within 2.1 to 2.9 dB between 1 and 20 kHz.

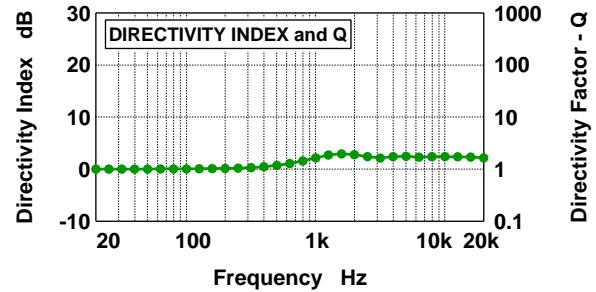


Fig. 19. Directivity index (left scale) and Q (right scale) of the CBT array of Fig. 15.

Figure 20 shows the on-axis loss of the broad-coverage CBT array. The CBT curved-line array exhibits loss above 1 kHz due to the curvature of the array. Above 1 kHz, the on-axis response rolls off at 10 dB/decade, because the sources are at different distances from the observation point.

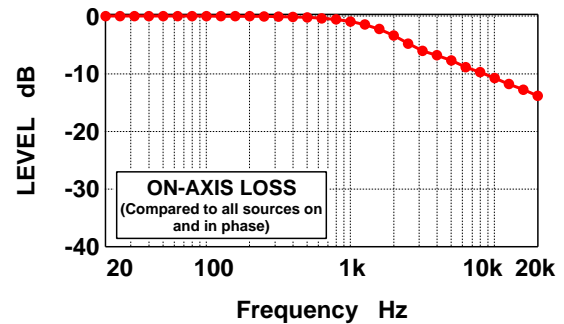


Fig. 20. On-axis loss of the CBT array of Fig. 15. The CBT array exhibits loss above 1 kHz due to the curvature of the array.

#### 4.2. Broad Vertical Coverage CBT Balloon Plots

The following polar balloons illustrate the 3D directional radiation of the curved-line CBT array of Fig. 15 at a frequency of 8 kHz. This high frequency was chosen to properly display all the features of the array’s radiation. Refer to Section 9 Appendix 2 for a complete set of balloons at octave centers from 500 Hz to 16 kHz.

The balloons are generated by calculating the response every 5° in azimuth (longitude) and every 1.25° in elevation (latitude). Figures 21 – 24 show respectively oblique, front, side, and top views of the balloon. Refer to Fig. 1 for color coding of the balloons.

The oblique view shown in Fig. 21 illustrates all the unusual features of the radiation pattern of the CBT curved-line array. The axis of the array points down and to the right (see Fig. 2 for orientation). Note several features of the display:

1. the smooth rounded surface of constant level in the forward (and rearward because the radiation is bi-directional) facing directions, which implies even coverage,
2. the reduction of vertical beamwidth as one gets farther off axis horizontally,
3. the very narrow vertical coverage at  $\pm 90^\circ$  off axis horizontally, and
4. the sharp reduction of level in the Y-Z plane (up-down and right-left) except for narrow high-level projections in the extreme lateral directions at  $\pm 90^\circ$  off-axis horizontally.

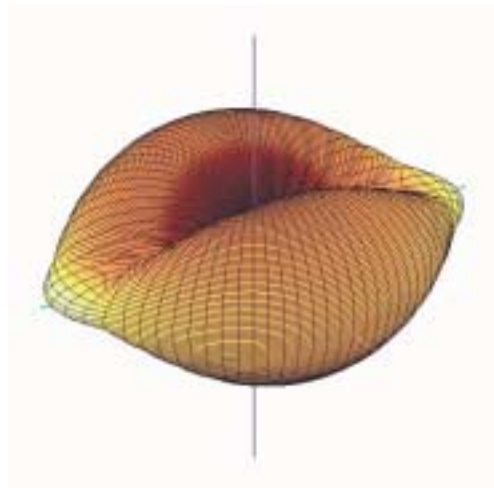


Fig. 21. Oblique view of the polar balloon of the  $140^\circ$  CBT line array of Fig. 15 at 8 kHz. Refer to Fig. 2 for axis orientation.

The front view shown in Fig. 22 illustrates the peculiar petal or eyeball shape of the radiation. Note that the highest levels of the radiation are at right angles ( $\pm 90^\circ$  horizontal) to the on-axis direction (which faces straight out of the page). Note also that these high-level directions are accompanied by very narrow vertical coverage (only about  $5^\circ$  at this frequency).

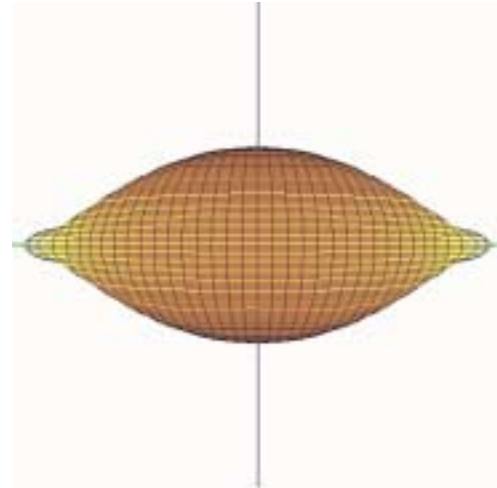


Fig. 22. Front view of the polar balloon of the  $140^\circ$  CBT line array of Fig. 15 at 8 kHz. The X axis points out of the page.

The side view shown in Fig. 23 illustrates the sharp reduction in level in the Y-Z plane (up-down and in-and-out of the page) and the dumb bell or petal shape of the pattern. Note also the high-intensity level and narrow vertical beamwidth at right angles to on axis (in-and-out of the page).

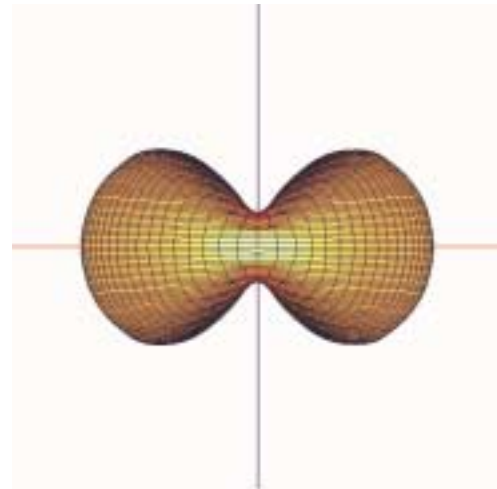


Fig. 23. Side view of the polar balloon of the  $140^\circ$  CBT line array of Fig. 15 at 8 kHz. The X axis points to the right.

The top view of Fig. 24 again shows clearly the high-intensity nubs (right-left) at right angles to on axis (up-down). As with all CBT arrays composed of point sources, the top view illustrates the forward-reverse symmetry of the CBT radiation.

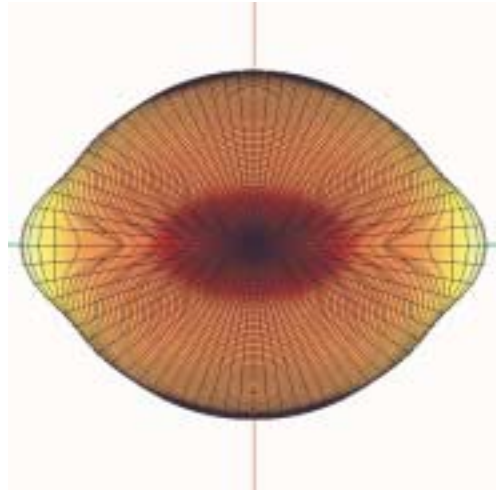


Fig. 24. Top view of the polar balloon of the 140° CBT line array of Fig. 15 at 8 kHz. The X axis points down and the Z axis points out of the page. Note that the highest levels of the radiation pattern are at right angles ( $\pm 90^\circ$  horizontal, right-left in this display) to the defined on-axis direction (up or down in the display).

### 4.3. Narrow Vertical Coverage CBT Array

This array is designed to provide a narrow vertical coverage of  $22.5^\circ$  on axis at frequencies above 1 kHz. The array is composed of 200 point sources equally distributed around a  $35^\circ$  circular arc of 1.37m (54") height located on the Z-X plane. The center of curvature of the arc is located at the origin. The arc's radius is 2.28m (89.79").

Because of the narrow vertical coverage of this array (which is one fourth that of the previous array), the height of the array is made four times that of the previous array in order to control vertical beamwidth down to the same frequency. This array is one wavelength high at 250 Hz or four wavelengths at 1 kHz. The close spacing of the sources insures that the line essentially behaves continuously up to 20 kHz.

Figures 25 to 27 respectively show side, front, and top views of the array.

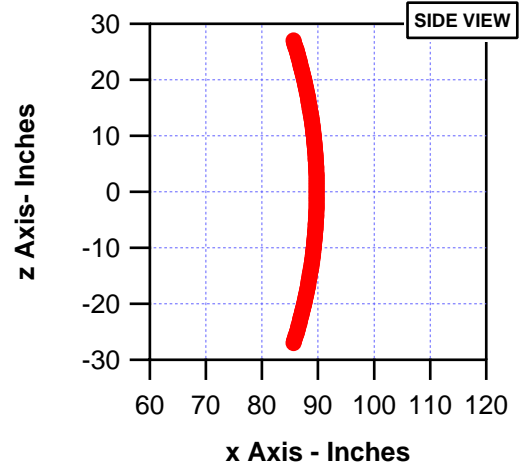


Fig. 25. Side view of a  $35^\circ$  CBT line array providing a vertical coverage of  $22.5^\circ$  made up of 200 point sources. The array is 1.37m (54") high (four wavelengths at 1 kHz). The array's center of curvature is located at the origin. The array points to the right in the direction of the positive X axis.



Fig. 26. Front view of the CBT array of Fig. 25.

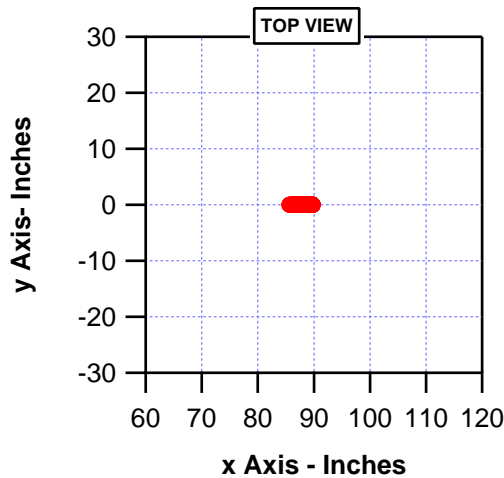


Fig. 27. Top view of the CBT array of Fig. 25.

Figure 28 shows the predicted vertical and horizontal beamwidth (-6 dB) of the narrow vertical coverage array. Note the extremely uniform vertical beamwidth of the array above 1 kHz. As before, although the horizontal beamwidth is constant at 360°, this does not imply that the horizontal coverage is independent of direction in the horizontal plane.

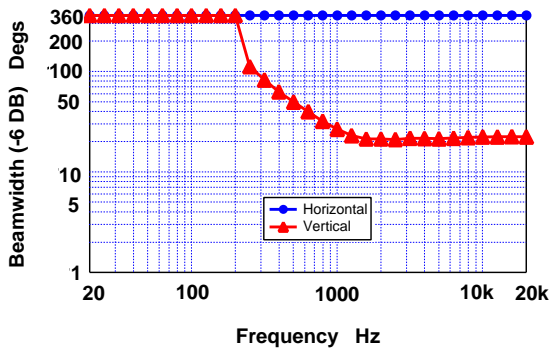


Fig. 28. Horizontal and vertical beamwidth (-6 dB) of the CBT array of Fig. 25.

Figure 29 indicates the CBT array’s predicted directivity as a function of frequency. The directivity is quite uniform above 1 kHz, fitting within a 7.2 to 8.7 dB window between 1 and 20 kHz. .

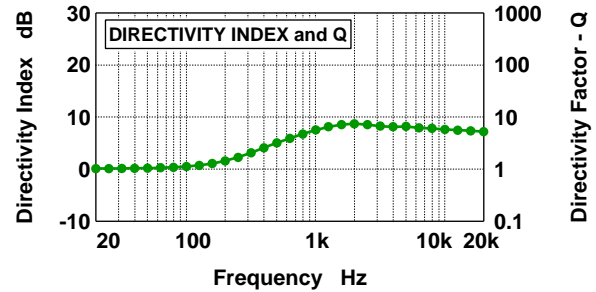


Fig. 29. Directivity index (left scale) and Q (right scale) of the CBT array of Fig. 25.

Figure 30 shows the on-axis loss of the narrow-coverage CBT array. The CBT curved-line array exhibits loss above 1 kHz due to the curvature of the array. Above 1 kHz, the on-axis response rolls off at 10 dB/decade. Note that this figure is identical to the on-axis loss of the previous array (Fig. 20), because the operating bandwidths of the two are identical.

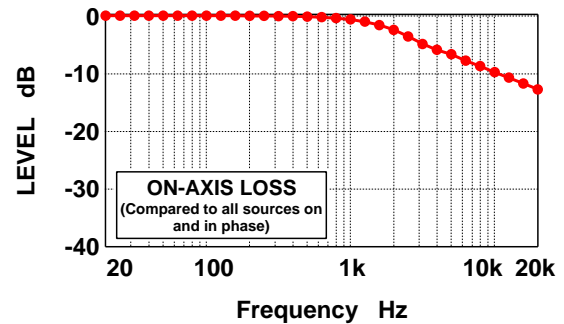


Fig. 30. On-axis loss of the array of Fig. 25. Note that the loss of this array is identical to the previous array (Fig. 20) because they both operate over the same frequency range.

#### 4.4. Narrow Vertical Coverage CBT Balloon Plots

The following polar balloons illustrate the 3D directional radiation of the curved-line CBT array of Fig. 25 at a frequency of 8 kHz. This high frequency was chosen to properly display all the features of the array’s radiation. Refer to Section 9 Appendix 2 for a complete set of balloons at octave centers from 500 Hz to 16 kHz.

The balloons are generated by calculating the response every 5° in azimuth (longitude) and every 1.25° in elevation (latitude). Figures 31 – 34 show respectively oblique, front, side, and top views of the balloon. Refer to Fig. 1 for color coding of the balloons.

The oblique view shown in Fig. 31 illustrates all the unusual features of the radiation pattern of the CBT curved-line array. Refer to the previous comments about the unusual features of these radiation patterns listed for Fig. 21 in section 4.2.

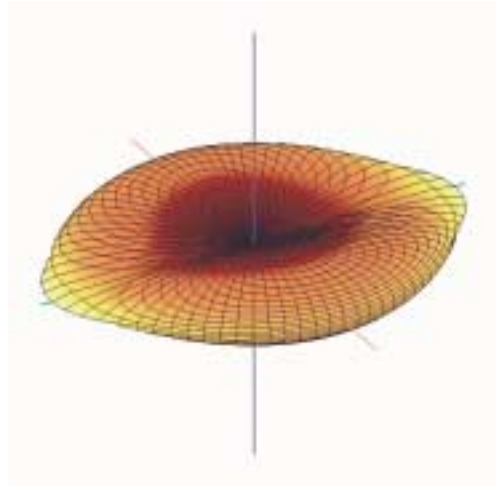


Fig. 31. Oblique view of the polar balloon of the 35° CBT line array of Fig. 25 at 8 kHz. Refer to Fig. 2 for axis orientation.

Fig. 32 illustrates the peculiar petal or eyeball shape of the forward radiation. Refer to text comments on Fig. 22. Note the extreme narrow coverage to the sides.

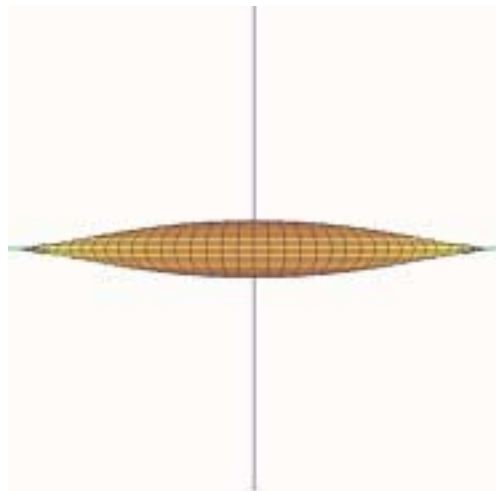


Fig. 32. Front view of the polar balloon of the 35° CBT line array of Fig. 25 at 8 kHz. The X axis points out of the page.

The side view shown in Fig. 33 illustrates much the same features as Fig. 23 and described previously in the text for that figure.

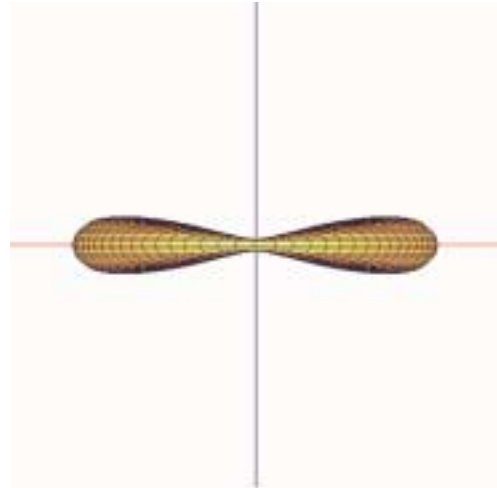


Fig. 33. Side view of the polar balloon of the 35° CBT line array of Fig. 25 at 8 kHz. The X axis points to the right.

The top view in Fig. 34 also illustrates much the same features as the previous Fig. 24, which are listed in the text for that figure.

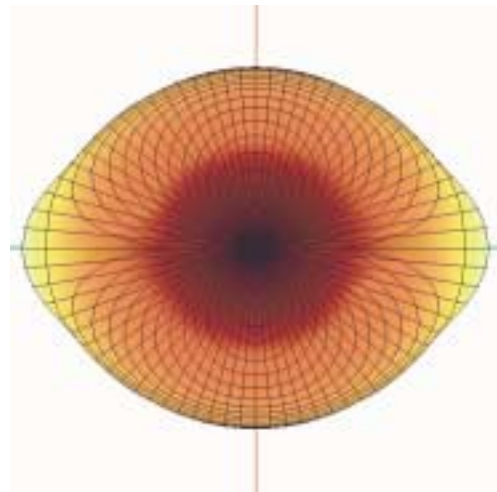


Fig. 34. Top view of the polar balloon of the 35° CBT line array of Fig. 25 at 8 kHz. The X axis points down and the Z axis points out of the page.

## 5. VARIATION OF CBT LINE ARRAY VERTICAL BEAMWIDTH WITH AZIMUTH ANGLE

This section analyzes the variation of vertical beamwidth with horizontal (azimuth) angle. The broad vertical coverage CBT array of Fig. 15 was analyzed in the following. The vertical beamwidth data was found to fit a cosine variation of the horizontal angle.

### 5.1. Simulate Vertical Beamwidth at Different Horizontal Off-Axis Angles

The broad vertical coverage CBT array of Fig. 15 was analyzed to generate several beamwidth vs. frequency plots at several off-axis horizontal directions including: 0, ±15°, ±30°, ±45°, ±60°, ±75°, ±80°, ±85°, and ±90°. These plots are shown in Fig. 35. The plots show that the vertical beamwidth progressively diminishes as you progress off axis horizontally.

At ±90° off axis, the curved-line array essentially appears as a straight-line array whose vertical beamwidth continually decreases with frequency. This decreasing beamwidth vs. frequency characteristic acts as an asymptote for the vertical beamwidth plots at intermediate horizontal off-axis angles.

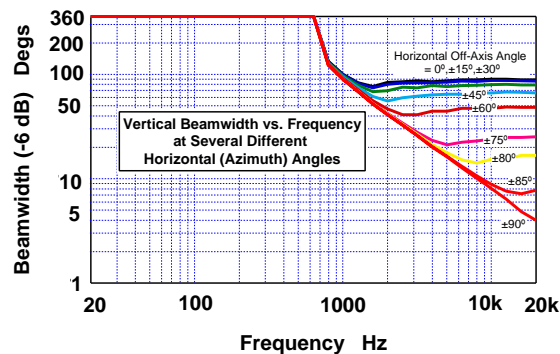


Fig. 35. Plot of the vertical beamwidth (-6 dB) vs. frequency at several different horizontal (azimuth) off-axis angles for the broad-coverage CBT line array of Fig. 15. Note that the vertical beamwidth of the array narrows as you go off axis horizontally. Note also that the vertical beamwidth only narrows to an asymptote that represents the beamwidth vs. frequency of a straight-line array of the same height as the CBT array.

Figure 36 shows the beamwidth values at the listed horizontal off-axis angles of Fig. 35 at the frequency

of 16 kHz (red dotted curve). The blue non-dotted curve shows the best-fit cosine variation curve for an initial angle of 92.5°. This data shows that the vertical beamwidth of the curved-line CBT array essentially follows a cosine variation decrease with off-axis horizontal angle.

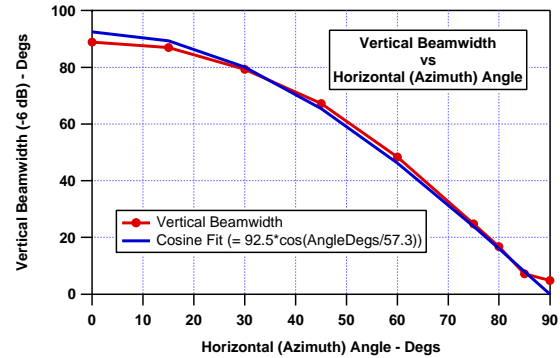


Fig. 36. Comparison of the vertical beamwidth data of Fig. 35 at 16 kHz and a cosine variation best fit.

### 5.2. Frontal Beam Shape

Assuming a cosine variation of vertical beamwidth with horizontal off-axis angle, as determined in the previous section, a frontal beam shape can be derived. This is shown in the following figure (Fig. 37).

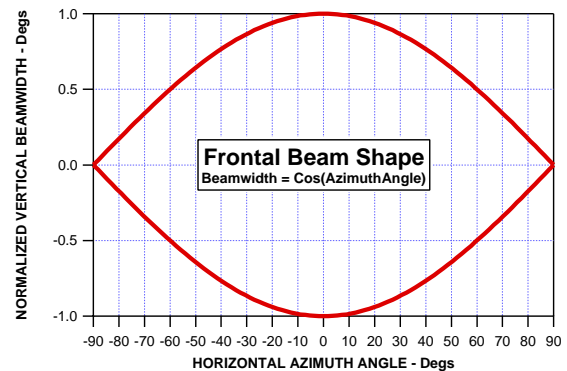


Fig. 37. Theoretical frontal beam shape of a CBT curved line array which looks somewhat petal- or eye-shaped. The plot reflects how the vertical beamwidth of the CBT array changes as a function of the horizontal azimuth angle. The vertical beamwidth of the CBT array progressively narrows as you go off axis horizontally reaching a small value at right angles to on axis (±90° off-axis horizontal) and follows a cosine relationship. Compare with Figs. 22 and 32.

## 6. CONCLUSIONS

This paper has investigated the 3D radiation pattern of the CBT curved-line circular-arc array through simulations based on arrays of point sources. It has shown that the radiation pattern is completely unlike the pattern of a conventional straight-line array that exhibits controlled vertical coverage but completely un-controlled omni-directional horizontal coverage with a pattern that is symmetric around the vertical axis.

Although still a line source, the CBT curved-line array exhibits significant horizontal directivity in addition to its expected vertical control. This horizontal directivity is exhibited by its variation of vertical beamwidth with horizontal off-axis angle. The vertical beamwidth varies smoothly from full value on axis to a low minimum value at right angles to the arrays forward axis in a manner that follows the cosine of the off-axis horizontal angle.

Interestingly, the curved-line array provides its maximum intensity at right angles ( $\pm 90^\circ$  off-axis horizontally) to its primary defined axis. This is because all the sources that make up the array are essentially equidistant from the observation point and hence in phase at these angles. This feature however, does not upset the controlled and smooth frontal coverage and directivity of the array because these regions of highest level are confined to very small regions on the sides of the radiation pattern.

The CBT curved-line array provides surprisingly constant directivity and uniform vertical beamwidth above a frequency related to the size of the array and its vertical coverage angle. This is accomplished without any complicated frequency-dependent signal processing. The only processing required is simple frequency-independent gain adjustment of the levels of the individual drivers to accomplish the Legendre shading.

## 7. REFERENCES

- [1] P. H. Rogers, and A. L. Van Buren, "New Approach to a Constant Beamwidth Transducer," *J. Acous. Soc. Am.*, vol. 64, no. 1, pp. 38-43 (1978 July).
- [2] A. L. Van Buren, L. D. Luker, M. D. Jevnager, and A. C. Tims, "Experimental Constant Beamwidth Transducer," *J. Acous. Soc. Am.*, vol. 73, no. 6, pp. 2200-2209 (1983 June).
- [3] D. B. Keele, Jr., "The Application of Broadband Constant Beamwidth Transducer (CBT) Theory to Loudspeaker Arrays," 109th Convention of the Audio Engineering Society, Preprint 5216 (Sept. 2000).
- [4] D. B. Keele, Jr., "Implementation of Straight-Line and Flat-Panel Constant Beamwidth Transducer (CBT) Loudspeaker Arrays Using Signal Delays," 113th Convention of the Audio Engineering Society, Preprint 5653 (Oct. 2002).

## 8. APPENDIX 1. REVIEW OF CBT THEORY

### 8.1. Conventional CBT Arrays

Quoting from Keele [3, Section 1]: "Rogers and Van Buren [1], and Buren et. al. [2] describe the theory and experiments of what they call broadband "constant beamwidth transducers" (CBT) for use as underwater projectors and receivers for sonar use. Here the transducer is in the form of a circular spherical cap of arbitrary half angle whose normal surface velocity (or pressure) is shaded with a Legendre function. The Legendre shading is independent of frequency. This transducer provides a broadband symmetrical directional coverage whose beam pattern and directivity is essentially independent of frequency over all frequencies above a certain cutoff frequency, and also change very little with distance from the source. The transducer can be designed to cover any arbitrary coverage angle with a constant beamwidth that extends over an operating bandwidth which is, in theory, virtually unlimited."

“Rogers and Van Buren [1] determined that if the radial velocity (or equivalently the surface pressure) on the surface of a rigid sphere of radius  $a$  conforms to

$$u(\theta) = \begin{cases} P_\nu(\cos\theta) & \text{for } \theta \leq \theta_0 \\ 0 & \text{for } \theta > \theta_0 \end{cases} \quad (1)$$

where

- $u(\theta)$  = radial velocity distribution
- $\theta$  = elevation angle in spherical coordinates,  
( $\theta = 0$  is center of circular spherical cap)
- $\theta_0$  = half angle of spherical cap
- $P_\nu(x)$  = Legendre function of order  $\nu$  ( $\nu > 0$ ) of argument  $x$ ,

then an approximation to the farfield pressure pattern, above a cutoff frequency which depends on the size of the sphere and the wavelength, will be

$$p(\theta) = \begin{cases} P_\nu(\cos\theta) & \text{for } \theta \leq \theta_0 \\ 0 & \text{for } \theta > \theta_0 \end{cases} \quad (2)$$

where

$$p(\theta) = \text{radial pressure distribution.}$$

“This surprising result shows that the farfield sound pressure distribution is essentially equal to the pressure distribution on the surface of the sphere. Rogers and Van Buren also point out that because the surface pressure and velocity are nearly zero over the inactive part of the outside surface of the sphere, the part of the rigid spherical shell outside the spherical cap region can be removed without significantly changing the acoustic radiation. This means that the ideal constant beamwidth behavior of the spherical cap is retained even though the rest of the sphere is missing!”

“The Legendre function  $P_\nu(\cos\theta)$  is equal to one at  $\theta = 0$  and has its first zero at angle  $\theta = \theta_0$ , the half angle of the spherical cap. The Legendre function order ( $\nu$ ) is chosen so that its first zero occurs at the half angle of the spherical cap. Note that  $\nu$  is normally greater than one, and not necessarily an integer.”

“Rogers and Van Buren also point out that the constant beamwidth behaviour of a rigid spherical cap also applies as well to an acoustically transparent spherical shell. However the acoustic radiation is

bidirectional, generating the same beam pattern front and rear.”

“To sum up the advantages of the CBT I quote from [1]:

“We enumerate the expected properties of the CBT above cutoff:

- (1) Essentially constant beam pattern.
- (2) Very low sidelobes.
- (3) The surface distribution as well as the pressure distribution at all distances out to the farfield is approximately equal to the surface distribution. Thus in a sense, there is no nearfield.
- (4) Since both the surface velocity and surface pressure have the same dependence on  $\theta$ , the local specific acoustic impedance is independent of  $\theta$  (and equal to  $\rho_0 c$ ). Thus the entire transducer is uniformly loaded.”

Keele [3] extends the CBT theory to loudspeaker arrays and provides a simplified four-term series approximation to the Legendre shading of Eq. (1) which is acceptable over all useful Legendre orders:

$$U(x) \approx \begin{cases} 1 + 0.066x - 1.8x^2 + 0.743x^3 & \text{for } x \leq 1 \\ 0 & \text{for } x > 1 \end{cases} \quad (3)$$

where

$$x = \text{normalized angle} \left( \frac{\theta}{\theta_0} \right)$$

Note that this function is exactly 1 at  $x=0$  and 0 at  $x=1$  (where  $\theta = \theta_0$  the half cap angle). All the following simulations use eq. (3) as a substitute for the Legendre function of Eq. (1).

As pointed out in [3], the coverage angle (6-dB-down beamwidth) of the CBT array is approximately 64% of the cap angle or circular-arc angle.

## 8.2. Application of CBT Theory to Line Arrays

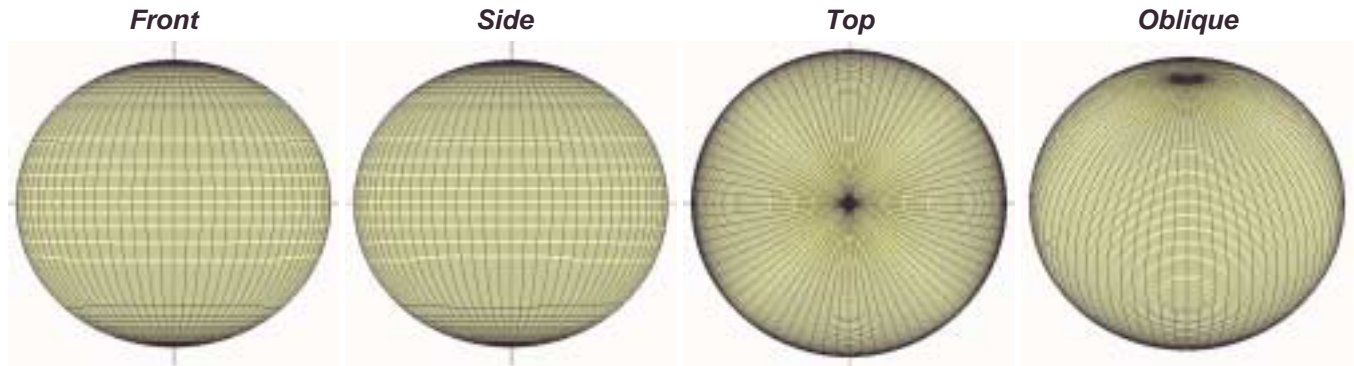
Keele [3] extended the CBT theory to circular-arc line arrays. Here the array is a circular-arc or wedge, usually oriented with its long axis vertical. This current paper analyzes the 3D radiation pattern of this type of array.

**9. APPENDIX 2. FULL SET OF POLAR BALLOONS FOR THE CBT ARRAYS**

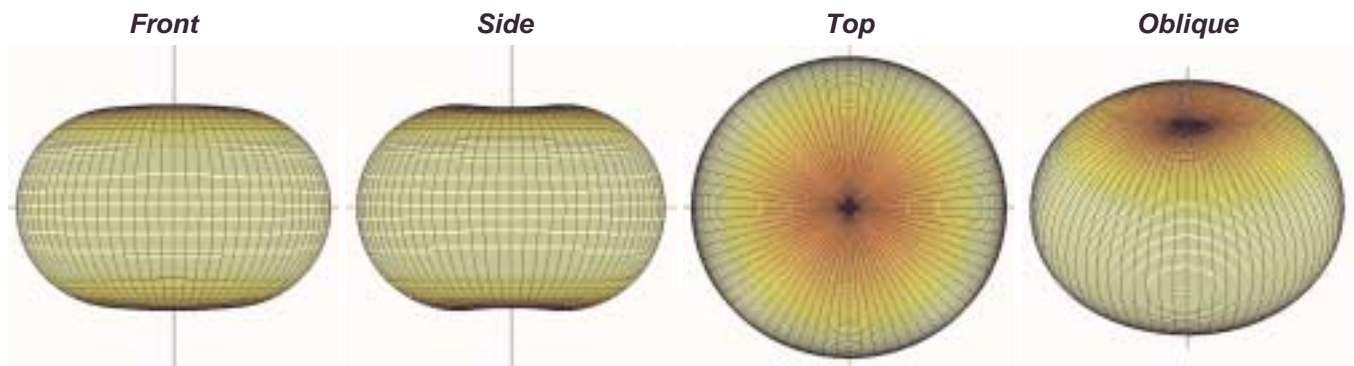
The following two sub sections show the predicted 3D polar response of the CBT arrays of Figs. 15 and 25. The polar balloons are calculated at every octave center frequency from 500 Hz to 16 kHz. The balloons are derived by calculating the response every 5° in azimuth (longitude) and every 1.25° in elevation (latitude). The array’s axis points in the direction of the positive X axis (towards the equator). Front, side, top, and oblique views are shown. Refer to Fig. 1 for the color scaling of these balloons and Fig. 2 for the axis orientation.

**9.1. Balloon Plots for the Broad Vertical Coverage CBT Line Array of Fig. 15.**

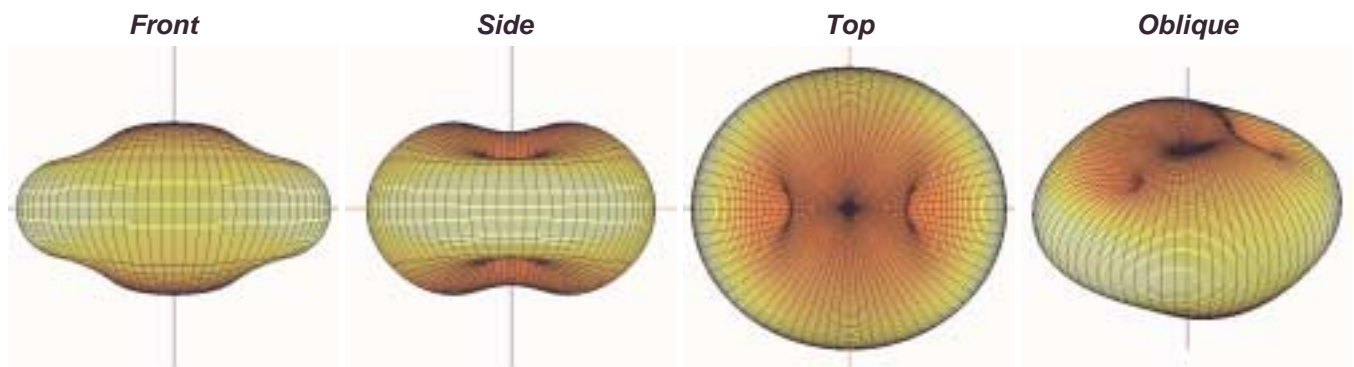
**500 Hz**



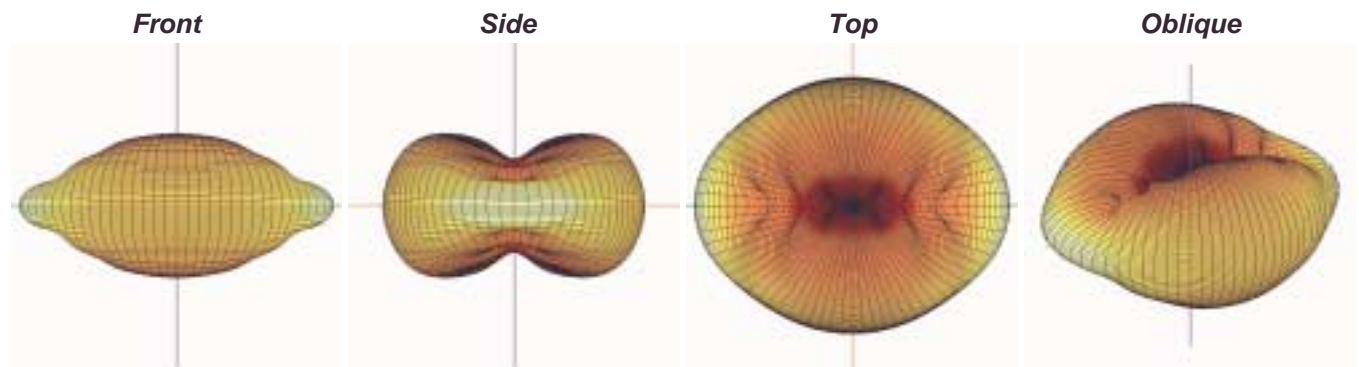
**1 kHz**



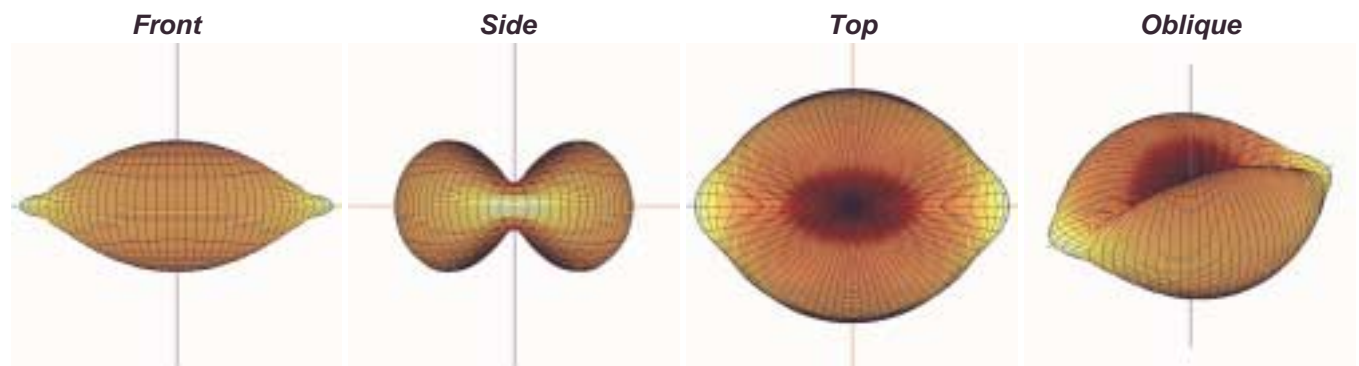
**2 kHz**



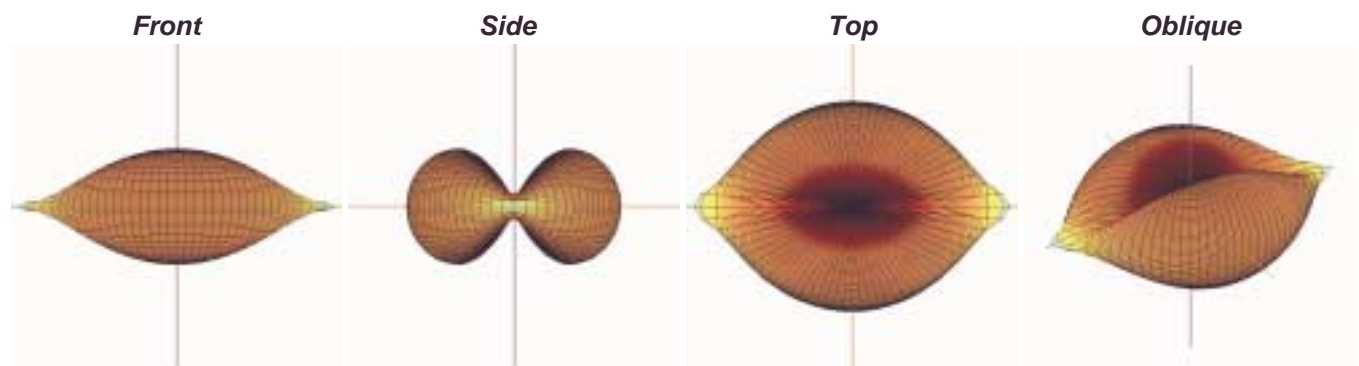
**4 kHz**



**8 kHz**

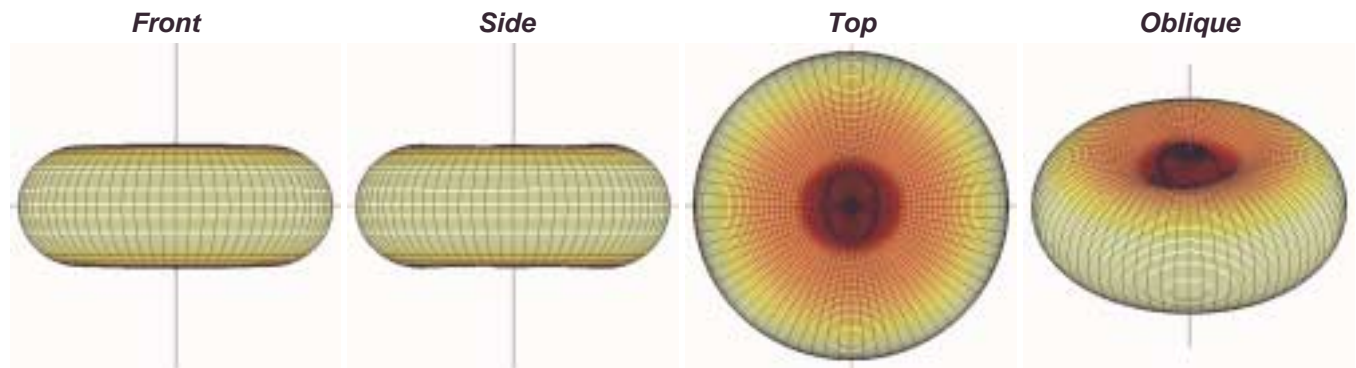


**16 kHz**

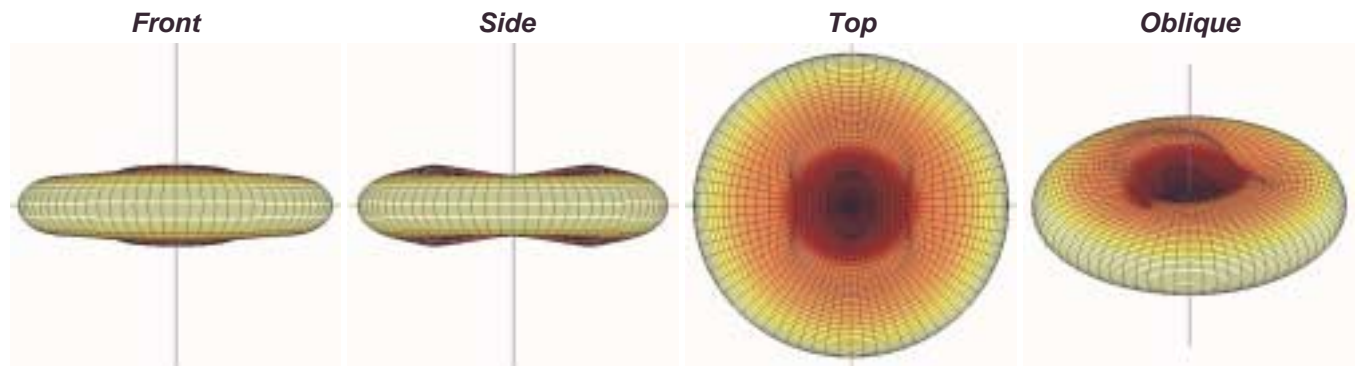


9.2. Balloon Plots for the Narrow Vertical Coverage CBT Line Array of Fig. 25.

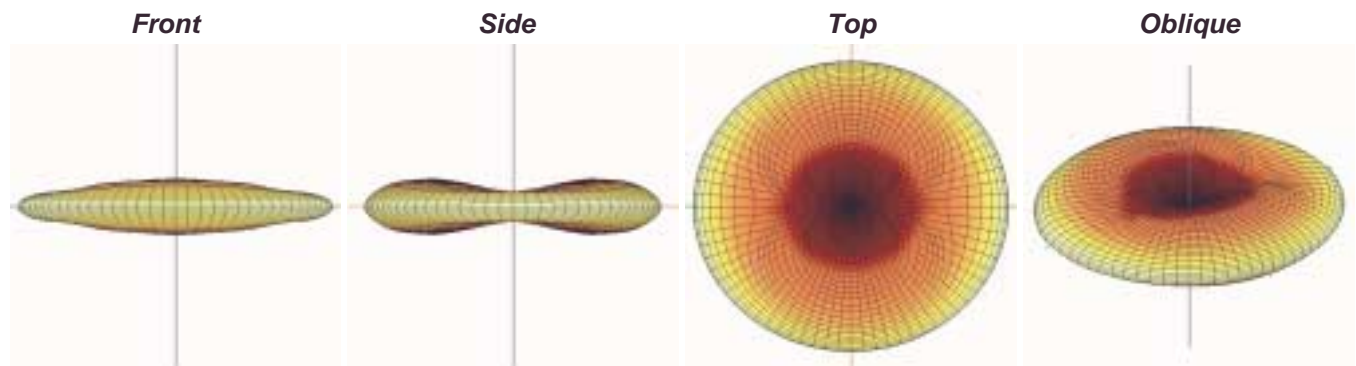
500 Hz



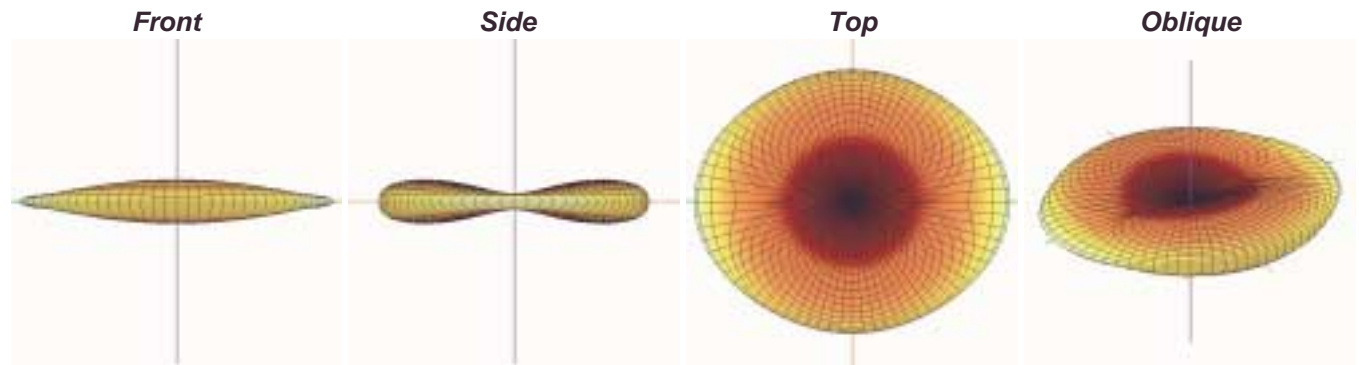
1 kHz



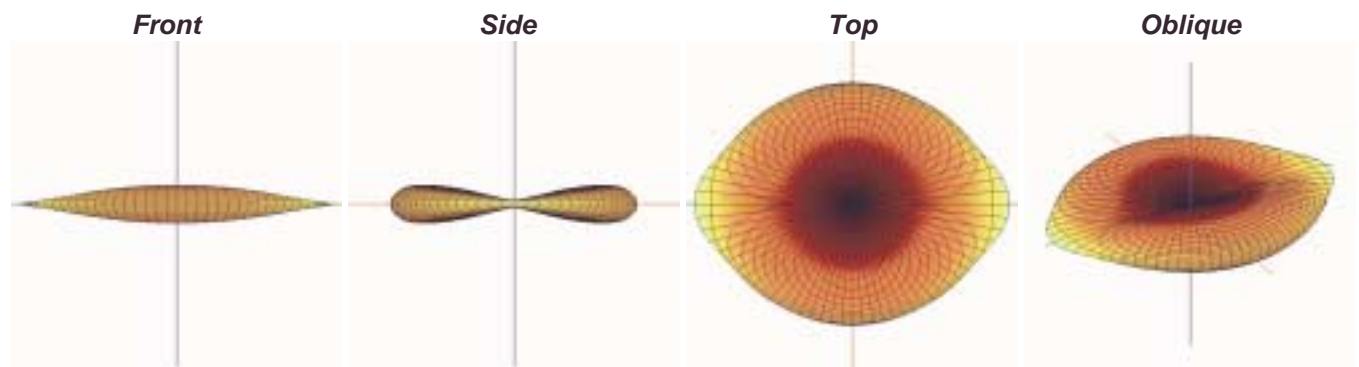
2 kHz



**4 kHz**



**8 kHz**



**16 kHz**

